Pseudo-symmetries of the Phases of $(Et_4N)_2ZnBr_4$

P. Sondergeld, H. Fuess, S. A. Mason[a], H. Ishihara[b], and W. W. Schmahl[c]

Institute of Materials Science, University of Technology, Darmstadt, Germany
[a] Institut Laue-Langevin, Grenoble, France
[b] Faculty of Education, Saga University, Japan
[c] Institut für Mineralogie, Ruhr-Universität Bochum, Germany

Reprint requests to Dr. P. S.; Institut für Experimentalphysik, Universität Wien, Strudlhofgasse 4, A-1090 Wien, E-mail: peso@merlin.ap.univie.ac.at

Z. Naturforsch. **55a,** 801–809 (2000); received August 2, 2000

The phase sequence of $(Et_4N)_2ZnBr_4$ has been determined based on thermal analysis. Below the decomposition point (572 K) four phases are distinguished.

The structures of three of the phases have been determined from 4-circle diffraction data at 240 (neutrons), 299 and 373 K (X-rays), respectively. The multiply twinned low-temperature phase (at 240 K) is characterized by a pseudo-orthorhombic lattice (monoclinic, P1a1, a = 17.6120(9) Å, b = 8.8195(4) Å, c = 16.1062(6) Å and β = 89.94(2)°), whereas the room-temperature phase (299 K: $P42_1c$, a = 8.9874(6) Å and c = 15.9774 Å) and the first high-temperature phase (373 K: $P4_2/nmc$, a = 9.145(4) Å and c = 15.835(8) Å) belong to the tetragonal crystal system. The transitions between the three phases are essentially connected with a stepwise ordering of the Et_4N^+ ions, whereas the positions of the heavy atoms change only slightly. Three ^{81}Br NQR lines are observed between 77 and 204 K.

Key words: $(Et_4N)_2ZnBr_4$; Twinning; Pseudo-symmetry; Structures.

Introduction

Many members of the A_2BX_4 (K_2SeO_4) family of crystals are well-known for the occurrence of ferroelectric and modulated phases [1]. Rb_2ZnBr_4, a representative of the tetrabromometallates, has six different phases including an incommensurate one at room temperature [2–4].

On replacing the Rb^+ ion by R_4N^+ (R = methly, ethyl, propyl, ...), a new family of compounds is created. In case of R = methyl both the tetrachloro- and -bromometallates can directly be derived from the β-K_2SO_4 type, whereas the phase transition behaviour already differs between these two types of compounds: Whereas many of these tetrachlorometallates have incommensurate phases, only $(Me_4N)_2CuBr_4$ is known to have one among the tetrabromometallates [5–6].

On increasing the alkyl chain length of the R_4N^+ ion, the spheroidal character of the ion is lost. The Et_4N^+ ion, for instance, can exist as one of three conformers: one of two mirror-image isomers in point group $\bar{4}$ (S_4) or in point group $\bar{4}2$ m (D_{2d}). The orientational disorder of this ion is also known from the transition behaviour of the binary salt Et_4NBr, resulting in a plastic high-temperature phase [7].

Stucky et al. [8] determined the room-temperature structure of $(Et_4N)_2NiCl_4$ in space group $P4_2/nmc$ with an orientational disorder of the Et_4N^+ ion. It seems reasonable to assume that several members of the group $(Et_4N)_2M^{II}Br_4$ (M^{II}: bivalent metal ion of the 3d series), particularly $(Et_4N)_2ZnBr_4$, have the same or at least a very similar room-temperature structure. The structure of $(Et_4N)_2NiCl_4$ cannot be derived from the β-K_2SO_4 type, which explains, partially, why no incommensurate phase transition has been found for this group of compounds yet.

Assuming $(Et_4N)_2ZnBr_4$ is isomorphous to $(Et_4N)_2NiCl_4$ at room temperature, the structure consists of isolated $[ZnBr_4]^{2-}$ tetrahedra and isolated Et_4N^+ ions in point group $\bar{4}$ (S_4), which is a prerequisite for a potential ferroelectric. Studies of the birefringence [9] reveal a second-order transition at ~ 311 K and a first-order transition around 281–283 K with a hysteresis of ~ 2 K.

Figure 1 shows the phase transition scheme that has been established based on the results of several groups. The transition temperatures and the decomposition point are from our own thermal analysis of the compound, including the discovery of an hitherto unknown high-temperature phase (phase 4). An additional anomaly around ~ 230 K, found by Kahrizi et al. [10] could not be confirmed.

Whereas the temperature dependence of some of the physical properties of $(Et_4N)_2ZnBr_4$ has already been studied [9–11], the structures of the four known phases have not been determined yet. The room-temperature

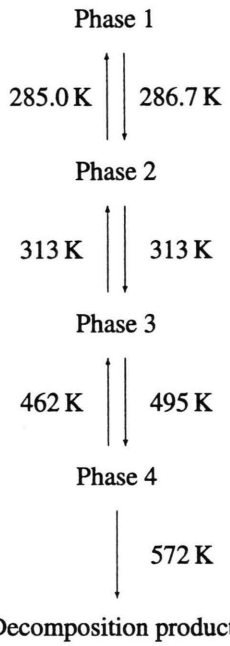

Fig. 1. Phase transition scheme of $(Et_4N)_2ZnBr_4$.

structure of a similar compound, $(Et_4N)_2CdBr_4$, was determined in another space group [12] than that of the tetrachloronickelate [8], with (partially) different Et_4N^+ conformers. It follows that the assumption of a general isomorphism of the compounds of the family $(Et_4N)_2M^{II}Br_4$ is definitely not true.

Table 1. Experimental details of the neutron and X-ray data collections and structure refinements of the phases 1–3 of $(Et_4N)_2ZnBr_4$.

Phase	1	2	3
Crystal size [mm^3]	2.8×2.3×2.4	0.45×0.45×0.49	0.46×0.53×0.57
Temperature [K]	240	299	373
μ [cm^{-1}]	D9: 233 D19: 3.03	69.92	68.14
(sin θ)/λ range	D9: 0.0802 ≤ (sin θ)/λ ≤ 0.4928 D19: 0.4928 ≤ (sin θ)/λ ≤ 0.6018	0.0626 ≤ (sin θ)/λ ≤ 0.5942	0.0631 ≤ (sin θ)/λ ≤ 0.5940
Index ranges	$-20 \le h \le 20$ $-10 \le k \le 10$ $-19 \le l \le 19$	$-10 \le h \le 0$ $-10 \le k \le 0$ $-19 \le l \le 0$	$-10 \le h \le 10$ $-10 \le k \le 10$ $-18 \le l \le 18$
Lattice parameters:			
a [Å]	17.6120 (9)	8.9874 (6)	9.1450 (44)
b [Å]	8.8195 (4)	8.9874 (6)	9.1459 (44)
c [Å]	16.1062 (6)	15.9774 (14)	15.8354 (81)
β [°]	89.94 (2)	90	90
V [Å^3]	2501.8 (3)	1290.5 (3)	1324 (2)
Space group	P1a1 (no. 7)	P$\bar{4}2_1$c (no. 114)	P4$_2$/nmc (no. 137)
Formula units Z	4	2	2
ϱ_{cal} [g cm^{-3}]	1.71	1.66	1.62
Reflections:			
all	5836	2552	5018
unique	3144	1140	665
unique, ($I>2\sigma(I)$)	2830	773	451
R_{int}	–	0.0471	0.0865
R_σ	0.0510	0.0356	0.0344
Final $R(I>2\sigma(I))$:			
R_1	0.0580	0.0383	0.0464
wR_2	0.1136	0.1011	0.1087
Final R(all data):			
R_1	0.0848	0.0687	0.0724
wR_2	0.1293	0.1212	0.1265
Goodness of fit on F^2	1.044	1.075	1.170

Experimental

The $(Et_4N)_2ZnBr_4$ crystals were obtained by dissolving stoichiometric amounts (2:1) of Et_4NBr and $ZnBr_2$ in boiling ethanol and slow evaporation of the solvent at ~40 °C.

TG and DTA measurements were performed simultaneously on a Setaram 92 using ~10 mg of $(Et_4N)_2ZnBr_4$ and a heating rate of 5 K min^{-1}. DSC measurements were performed on a Setaram 121 using ~50 mg of $(Et_4N)_2ZnBr_4$ and both cooling and heating rates of 5 and 1 K min^{-1}.

For the structure determination of $(Et_4N)_2ZnBr_4$ in phase 1 an isometric crystal (diameter: ~2.5 mm) was used and cooled down to 240 K. The data collection was carried out on the D9 and D19 4-circle diffractometers of the Institut Laue-Langevin (ILL), Grenoble. For the structure determination of $(Et_4N)_2ZnBr_4$ in the phases 2 and 3 two different crystals with diameters of ~0.5 mm were used. The data collections were carried out on a Stoe STADI 4 X-ray 4-circle diffractometer at room temperature (299 K) and 373 K, respectively. Details of the three measurements are presented in Table 1. The structures were solved by Patterson maps and refined by least-squares methods with the programs given in [13].

^{79,81}Br NQR measurements were carried out on a super-regenerative spectrometer (Decca type). Approximately 4 cm^3 of crystalline powder of $(Et_4N)_2ZnBr_4$ were sealed in a glass tube and cooled in a cold nitrogen gas stream. The sample was heated stepwise, starting at 77 K, while at various low-temperature points ^{79,81}Br NQR spectra were recorded.

Results

Thermal Analysis

Figure 2 shows the results of a combined DTA/TG measurement of the compound. The decomposition starts at 572.8 K (T_a). The analysis of the loss of weight (TG) can be divided into three steps. The first ($\sim T_a$) and the second step (finished at T_f) each imply a loss of weight corresponding to the mass of one formula unit of Et_4NBr and are therefore attributed to a stepwise loss of Et_4NBr. A partial loss of the second formula unit can be marked by the turning point at T_i. The entire loss of the second formula unit is completed at $T_f = 667.2$ K. It coincides with the melting point of $ZnBr_2$. The decomposition is finished at 768.2 K (T_e).

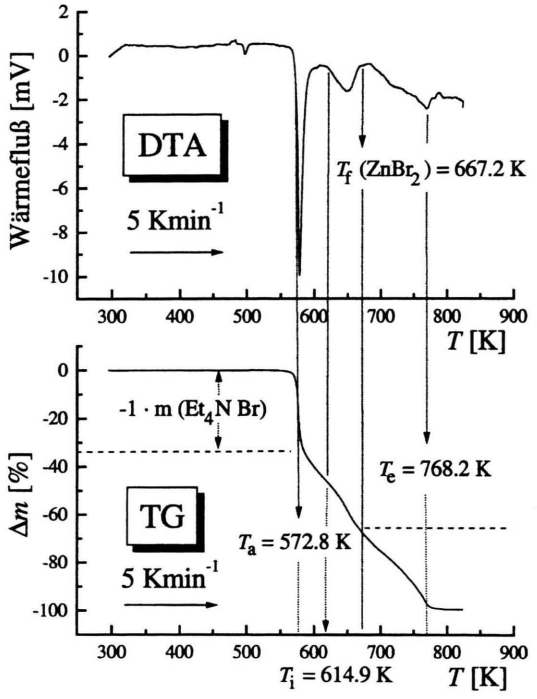

Fig. 2. DTA/TG analysis of $(Et_4N)_2ZnBr_4$ (heating rate: 5 K min^{-1}). The decomposition starts at T_a and is completed at T_e. The loss of the second formula unit of Et_4NBr can be subdivided by T_i into two more partial steps.

Table 2 summarises the results of the DSC measurements including the transformation enthalpy ΔH, the onset temperature T_a of the transition and the temperature T_{max} at the peak maximum. Assuming that the configurational entropy ΔS_c is more or less identical to the transformation entropy ΔS_t, we have

$$|\Delta S_c| = R \ln\left(\frac{\omega_{i+1}}{\omega_i}\right) \approx |\Delta S_t|. \quad (1)$$

The parameter $\omega_{i+1} : \omega_i$ corresponds to the ratio between the number of states, represented in this case by the multiplicities, above (ω_{i+1}) and below (ω_i) the temperature of transition i. Three different anomalies were found, and thus four different phases could be distinguished. The first transition is of slightly first order with a hysteresis range of 1.7 K (285–286.7 K). The second transition (at 313.2 K) is characterised by a step in the base line of the heat flow. Since neither a hysteresis nor a transformation enthalpy was observed in this case, it must be classified as a second-order transition. The third transition, by contrast, is clearly of first order with a hysteresis of 33.6 K (461.8–495.4 K).

Structure Determinations

The extinction rules of phase 3 (373 K) turned out to be "*hk*0: $h + k = 2n + 1$" and "*hhl*: $l = 2n + 1$" for a tetragonal crystal system. In this special case the space group must definitely be $P4_2/nmc$ (no. 137), which was confirmed by the structure solution using the heavy atom method. At room temperature (299 K, phase 2) the same extinction rules were observed for practically the same tetragonal lattice. However, the analysis of the difference fourier map revealed that the inner carbon atoms of the

Table 2. Results of the DSC measurements of $(Et_4N)_2ZnBr_4$, including the transformation enthalpy ΔH, the transformation entropy ΔS, the ratio $\omega_{i+1} : \omega_i$ of the multiplicities of the phases $i + 1$ and i, the onset temperature T_a and the temperature T_{max} at the peak maximum.

Transition	Mode	ΔH [J mol^{-1}]	T_a [K]	T_{max} [K]	ΔS [J mol^{-1} K^{-1}]	$\omega_{i+1} : \omega_i$
1	heating	−5032(75)	287(1)	289(1)	17.5(3)	8.2(3):1
	cooling	4998(82)	285(1)	283(1)	−17.5(3)	8.2(3):1
2	heating	–	313(1)	–	–	1:1
	cooling	–	313(1)	–	–	1:1
3	heating	−5573(145)	495(2)	500(2)	11.3(3)	3.9(2):1
	cooling	8624(223)	462(2)	457(2)	−18.7(5)	9.5(6):1

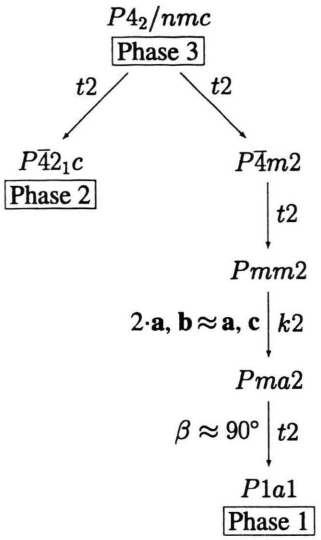

Fig. 3. Group-subgroup relations of the phases 1–3 of $(Et_4N)_2ZnBr_4$ after Bärnighausen [14].

Et_4N^+ ion could only be located in the maximal subgroup $P\bar{4}2_1c$ (no. 114), thus formally reducing the extinction rule "*hk*0: $h + k = 2n + 1$" to "*h*00: $h = 2n + 1$". All other atoms could be located using the space group symmetry $P4_2/nmc$. On cooling down to 240 K, superlattice reflections appeared with "*h* or *k* even" with regard to the common tetragonal lattice of the phases 2 and 3. This corresponds to an extinction rule "*h, k* odd". None of the known 230 space groups, particularly not a tetragonal one, has such an extinction rule. Instead the structure solution of phase 1 (240 K) could be carried out successfully in space group *P*1a1 (no. 7), which is a subgroup of $P4_2nmc$ (no. 137). In this case the unit cell is pseudo-orthorhombic with $a \approx 2b$ and $\beta \approx 90°$. The extinction rule turned out to be "*h*0*l*: $h = 2n + 1$", thus indicating the glide plane *a* perpendicular to the basis vector ***b***. Figure 3 shows the group-subgroup relations of the phases 1, 2, and 3 after Bärnighausen [14]. Both symmetry reductions from phase 3 to 2 and 1, respectively, involve a loss of the centre of inversion and thus racemic twinning. This has to be considered only if anomalous dispersion occurs, thus for the X-ray data of phase 2, but not for the neutron data of phase 1. In case of phase 2 a volume ratio of the two enantiomorphs of 1.17 : 1 was determined. Besides, the symmetry reduction from point group 4/mmm (phase 3) to point group m (phase 1) involves the transformation of the two mirror planes ‖ (1 1 0) and (1 $\bar{1}$ 0) into two twin planes. The four distinguishable twin components of phase 1 (240 K, neutrons), resulting from this twinning process, yielded volume ratios of 2.42:2.38:1.11:1 during the structure refinement of phase 1.

Table 3. Comparable unique sites with occupation factors (*Sof*) and equivalent isotropic displacement parameters U_{eq} of 11 non-hydrogen atoms of the phases 1–3 of $(Et_4N)_2ZnBr_4$. In case of phase 1 the *x*-values are multiplied by 2 with regard to the pseudo-orthorhombic cell ($a \approx 2b$, $\beta \approx 90°$). In case of phase 3 the co-ordinates are shifted by +1/4, –1/4, –1/4 with regard to the original refinement in space group $P4_2/nmc$.

Atom	Phase	*x*	*y*	*z*	*Sof*	U_{eq}
Zn(1)	1	1	1.0000(4)	1	1	0.0414(8)
	2	1	1	1	1/4	0.0622(1)
	3	1	1	1	1/4	0.0833(2)
Br(1)	1	0.7946(3)	0.9789(4)	1.0999(2)	1	0.0543(9)
	2	0.78311(3)	1.0009(1)	1.08738(2)	1	0.1057(1)
	3	0.78757(4)	1	1.08842(2)	1/2	0.1336(2)
N(1)	1	1.0084(4)	0.4914(2)	0.1709(1)	1	0.0363(4)
	2	1	1/2	0.1642(1)	1/2	0.0690(7)
	3	1	1/2	0.1642(2)	1/4	0.092(1)
C(1)	1	1.0750(4)	0.4253(4)	0.2511(2)	1	0.0546(9)
	2	0.963(1)	0.4409(6)	0.2442(3)	1/2	0.174(4)
	3	0.960(2)	0.4421(7)	0.2463(4)	1/4	0.179(5)
C(2)	1	1.0639(4)	0.2519(4)	0.2560(2)	1	0.0558(9)
	2	1.037(1)	0.2867(9)	0.2640(6)	1/2	0.176(5)
	3	1.034(3)	0.304(1)	0.2792(9)	1/4	0.283(9)
C(3)	1	1.0324(4)	0.6615(3)	0.1707(2)	1	0.0428(8)
	2	1.0142(9)	0.6649(6)	0.1704(3)	1/2	0.121(2)
	3	1.030(1)	0.6549(9)	0.1779(5)	1/4	0.194(3)
C(4)	1	0.9942(6)	0.7447(4)	0.2495(2)	1	0.075(1)
	2	1.0384(9)	0.7437(6)	0.2464(3)	1/2	0.104(2)
	3	1.035(1)	0.7366(7)	0.2504(4)	1/4	0.117(3)
C(5)	1	0.8394(4)	0.4553(4)	0.1681(2)	1	0.0530(9)
	2	0.8180(7)	0.497(2)	0.1614(4)	1/2	0.144(3)
	3	0.831(1)	1/2	0.1634(5)	1/4	0.242(7)
C(6)	1	0.7448(4)	0.5165(6)	0.0975(2)	1	0.090(1)
	2	0.7619(8)	0.490(2)	0.0906(3)	1/2	0.154(3)
	3	0.7597(7)	0.4593(9)	0.0816(5)	1/4	0.115(3)
C(7)	1	1.0696(4)	0.4250(4)	0.0916(1)	1	0.0495(9)
	2	1.0635(8)	0.4336(8)	0.0908(3)	1/2	0.112(3)
	3	1.0670(8)	0.4286(8)	0.0924(3)	1/4	0.117(3)
C(8)	1	1.2380(4)	0.4459(5)	0.0784(2)	1	0.075(1)
	2	1.2209(9)	0.487(2)	0.0524(6)	1/2	0.204(3)
	3	1.182(2)	1/2	0.050(1)	1/4	0.34(1)

Comparison of the Structures

Table 3 specifies comparable sites, site occupation factors (*Sof*) and equivalent isotropic displacement parameters (U_{eq}) of the non-hydrogen atoms of the asymmetric units of the phases 1–3. The co-ordinates of phase 3 are shifted by +1/4, –1/4, –1/4, and the *x*-values of the

Table 4. 35 unique sites of the non-hydrogen atoms of phase 1 with site occupation factors (*Sof*) and equivalent isotropic displacement parameters U_{eq}. These positions complement the 11 sites of phase 1 given in table 3 to a full set of the asymmetric unit of this phase. The *x*-values of the co-ordinates refer to the pseudo-orthorhombic cell ($a \approx 2\,b$, $\beta \approx 90°$).

Atom	Phase	*x*	*y*	*z*	*Sof*	U_{eq}
Br(2)	1	0.6197(2)	1.0080(3)	1.0826(2)	1	0.0444(7)
Br(3)	1	0.4922(2)	1.2491(5)	0.9301(2)	1	0.065(1)
Br(4)	1	0.4994(2)	0.8011(4)	0.9069(2)	1	0.064(1)
Zn(2)	1	0.7615(2)	0.5063(4)	0.5022(2)	1	0.0408(9)
Br(5)	1	0.8705(2)	0.4710(4)	0.4105(2)	1	0.0518(9)
Br(6)	1	0.6440(2)	0.5024(4)	0.4329(2)	1	0.0530(9)
Br(7)	1	0.7737(2)	0.7413(3)	0.5758(2)	1	0.0429(8)
Br(8)	1	0.7678(2)	0.2928(4)	0.6022(2)	1	0.0505(9)
N(2)	1	0.5143(1)	0.5397(2)	0.66490(9)	1	0.0351(5)
C(9)	1	0.4937(2)	0.7098(3)	0.6657(2)	1	0.0463(7)
C(10)	1	0.5258(2)	0.7932(4)	0.5908(2)	1	0.066(1)
C(11)	1	0.4802(2)	0.4592(3)	0.5922(1)	1	0.0389(8)
C(12)	1	0.4947(2)	0.2893(3)	0.5827(2)	1	0.0555(9)
C(13)	1	0.6001(1)	0.5299(3)	0.6643(2)	1	0.0358(7)
C(14)	1	0.6384(2)	0.6039(4)	0.7363(2)	1	0.0528(9)
C(15)	1	0.4851(2)	0.4728(4)	0.7460(1)	1	0.0456(8)
C(16)	1	0.3943(2)	0.4642(4)	0.7529(2)	1	0.0559(9)
N(3)	1	0.7595(1)	1.0064(2)	0.3381(1)	1	0.0366(5)
C(17)	1	0.8464(2)	1.0398(4)	0.3326(2)	1	0.056(1)
C(18)	1	0.8933(2)	0.9670(5)	0.4026(2)	1	0.073(1)
C(19)	1	0.7409(3)	0.8350(4)	0.3419(2)	1	0.066(1)
C(20)	1	0.7694(2)	0.7546(4)	0.2638(3)	1	0.067(1)
C(21)	1	0.7267(2)	1.0760(4)	0.4164(2)	1	0.052(1)
C(22)	1	0.6417(2)	1.0658(5)	0.4265(2)	1	0.068(1)
C(23)	1	0.7263(2)	1.0739(4)	0.2617(2)	1	0.0531(9)
C(24)	1	0.7261(3)	1.2475(4)	0.2576(3)	1	0.072(1)
N(4)	1	0.2517(1)	0.9612(2)	0.8383(1)	1	0.0352(5)
C(25)	1	0.2811(2)	1.0380(4)	0.9191(2)	1	0.0511(9)
C(26)	1	0.2648(3)	1.2136(5)	0.9194(3)	1	0.070(1)
C(27)	1	0.2851(2)	0.0270(4)	0.7616(1)	1	0.0429(8)
C(28)	1	0.3669(2)	1.0307(4)	0.7534(2)	1	0.0475(9)
C(29)	1	0.2788(2)	0.8019(4)	0.8448(2)	1	0.055(1)
C(30)	1	0.2432(3)	0.7029(5)	0.9146(3)	1	0.086(2)
C(31)	1	0.1672(2)	0.9868(4)	0.8378(2)	1	0.0468(9)
C(32)	1	0.1238(2)	0.9123(6)	0.7657(2)	1	0.077(1)

atom positions in phase 1 refer to the pseudo-tetragonal lattice, i.e. the *x*-values are twice as large as those of the original refinement (pseudo-orthorhombic cell, $a \approx 2\,b$). Table 4 lists the remaining sites and equivalent isotropic displacement parameters of the non-hydrogen atoms of the asymmetric unit of phase 1 with regard to the pseudo-orthorhombic cell. The structure determinations were done without restraints and by refining all non-hydrogen atoms of the pseudo-orthorhombic cell anisotropically. In case of phase 1, in addition, all 80 hydrogen atoms of the asymmetric unit were refined isotropically.

The structure of phase 1 can be described by two different layers arranged parallel to the (001) net plane and defined by the *z*-values of the positions of Zn(1) and Zn(2), respectively. Figure 4(a) shows the first kind of layer with $z(\mathrm{Zn}(1)) = 1$ (or 0). The $[\mathrm{Zn}(1)\mathrm{Br}_4]^{2-}$ ion is surrounded by four Et_4N^+ ions (central atoms: N(1) and N(4)), the centres of gravity of which are situated about 1/6 **c** above and below the layer, respectively. Figure 4(b) shows the second kind of layer with $z(\mathrm{Zn}(2)) \approx 0.5$ and the $[\mathrm{Zn}(2)\mathrm{Br}_4]^{2-}$ ion surrounded by four Et_4N^+ ions, too, this time with the central atoms N(2) and N(3). Again their centres of gravity are situated about 1/6 **c** above and below this plane. The $[ZnBr_4]^{2-}$ co-ordination polyhedra are nearly tetrahedral with an average Zn–Br distance of 2.42 Å. All of the Et_4N^+ are mirror-image isomers (approximate point group $\bar{4}$) with the rotoinversion axes being arranged ∥ the (001) net plane. The Et_4N^+ ion can be regarded in terms of two different co-ordination spheres around the central nitrogen atom with an average N–C distance of 1.52 Å for the inner carbon atoms in a nearly tetrahedral arrangement. The outer carbon atoms have an average N–C distance of 2.58 Å and form tetrahedra as well, though slightly distorted.

The structures of the phases 2 and 3 are very similar to that of phase 1, as can be seen from Table 3. From one phase to another the positions of the central Zn and N atoms change only slightly. On the other hand, the two transitions phase 1 → phase 2 and phase 2 → phase 3 involve a change of the special site symmetry of both the $[ZnBr_4]^{2-}$ and the Et_4N^+ ions. Figure 5 shows the influence of the change of the special site symmetry on the Et_4N^+ ion. At 240 K (phase 1, Fig. 4(a) and (b)) the Et_4N^+ ion is ordered without any special site symmetry, the shape of the molecular ion is rather undistorted and the thermal ellipsoids (probability density: 50%) are rather small. The H atoms are arranged in the expected staggered conformation. At 299 K (phase 2, Fig. 4(c)) the Et_4N^+ ion is twofold disordered with the N atom being situated on a twofold rotation axis along 1,1/2, *z*. The ORTEP plot of the asymmetric unit (Fig. 4(d)) shows that many of the anisotropic displacement factors are quite large and the Et_4N^+ ion is clearly distorted. At 373 K (phase 3, Fig. 4(e)) the special site symmetry of the Et_4N^+ ion is mm 2 and the ion is fourfold disordered. The ORTEP plot (Fig. 4(f)) of the asymmetric unit of the ion shows even larger anisotropic displacement parameters than that of phase 2 (Fig. 4(d)). It is reasonable to assume that the obvious orientational disorder of the Et_4N^+ ions also affects the $[ZnBr_4]^{2-}$ ions. These have special site symmetries of 1 (phase 1), $\bar{4}$ (phase 2) and $\bar{4}$m2 (phase 3). Since the equivalent isotropic displacement parameter of Br(1) is still below 0.15 at 373 K (cf. Table 3), a resolution of the respective split positions is not present-

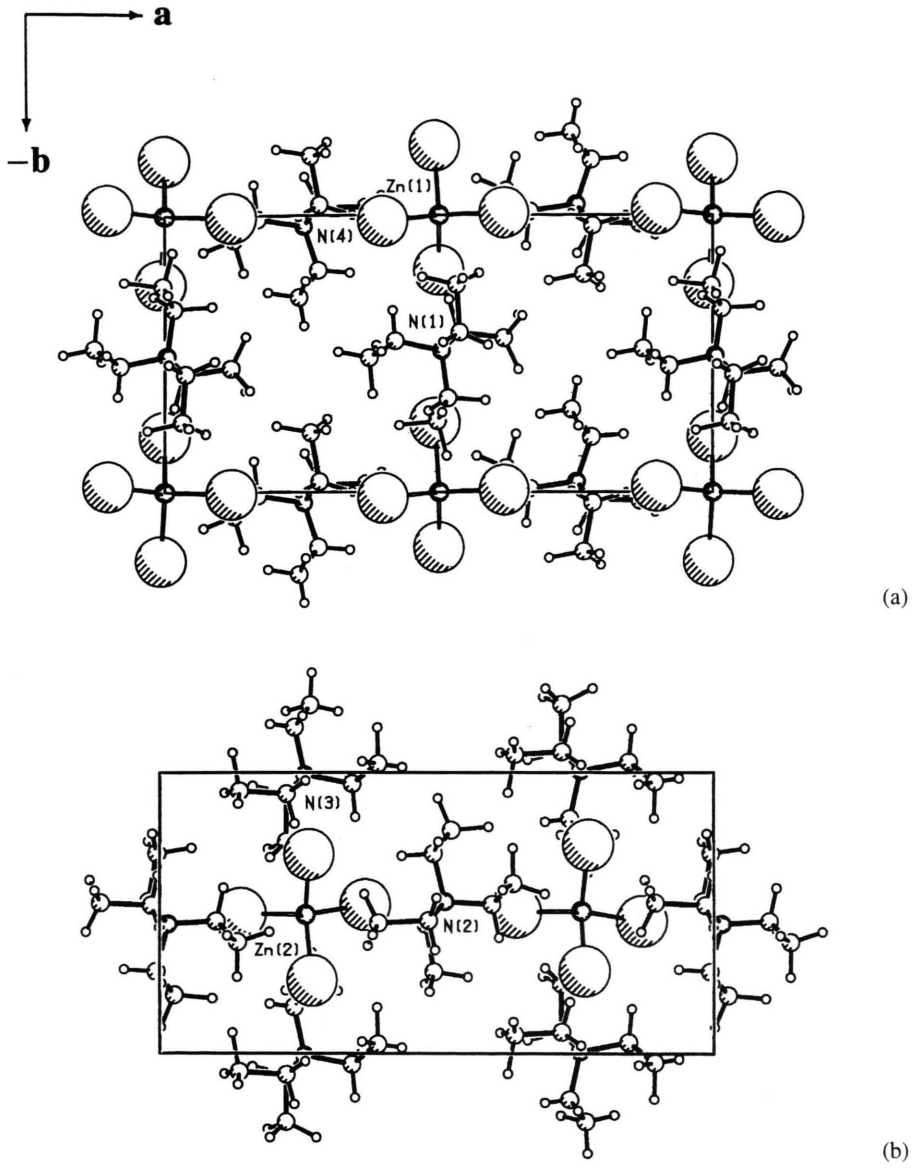

Fig. 4. Ball-stick model of the structure of phase 1 of $(Et_4N)_2ZnBr_4$, looking along the basis vector $\boldsymbol{c}$. The structure can be divided into two different layers perpendicular to the basis vector $\boldsymbol{c}$. The first layer (a) includes the positions of Zn(1) with $-0.2 \leq z \leq 0.2$, the second layer (b) the positions of Zn(2) with $0.3 \leq z \leq 0.7$.

Table 5. Results of the polynomial fitting to the temperature dependences of the three observed ^{81}Br NQR signals. For the fitting the equation $\nu_i(T) = \sum_{i=-1}^{2} a_i T^i$ was used where ν_i is the observed frequency and a_i an empirical coefficient of the signal i.

ν_i [MHz]	a_{-1}/MHz K	a_0/MHz	a_1/MHz K^{-1}	a_1/MHz K^{-2}
ν_1	21(12)	65.1(3)	0.005(2)	−0.000031(6)
ν_2	−68(14)	67.2(4)	−0.015(3)	0.000014(7)
ν_3	−19(18)	65.4(4)	−0.0061(4)	−0.000009(9)

ed here. These split positions are expected to be closer than 0.5 Å to one another.

NQR Spectroscopy

Figure 6 shows the results of the NQR measurements. For simplicity, only ^{81}Br NQR data are present-

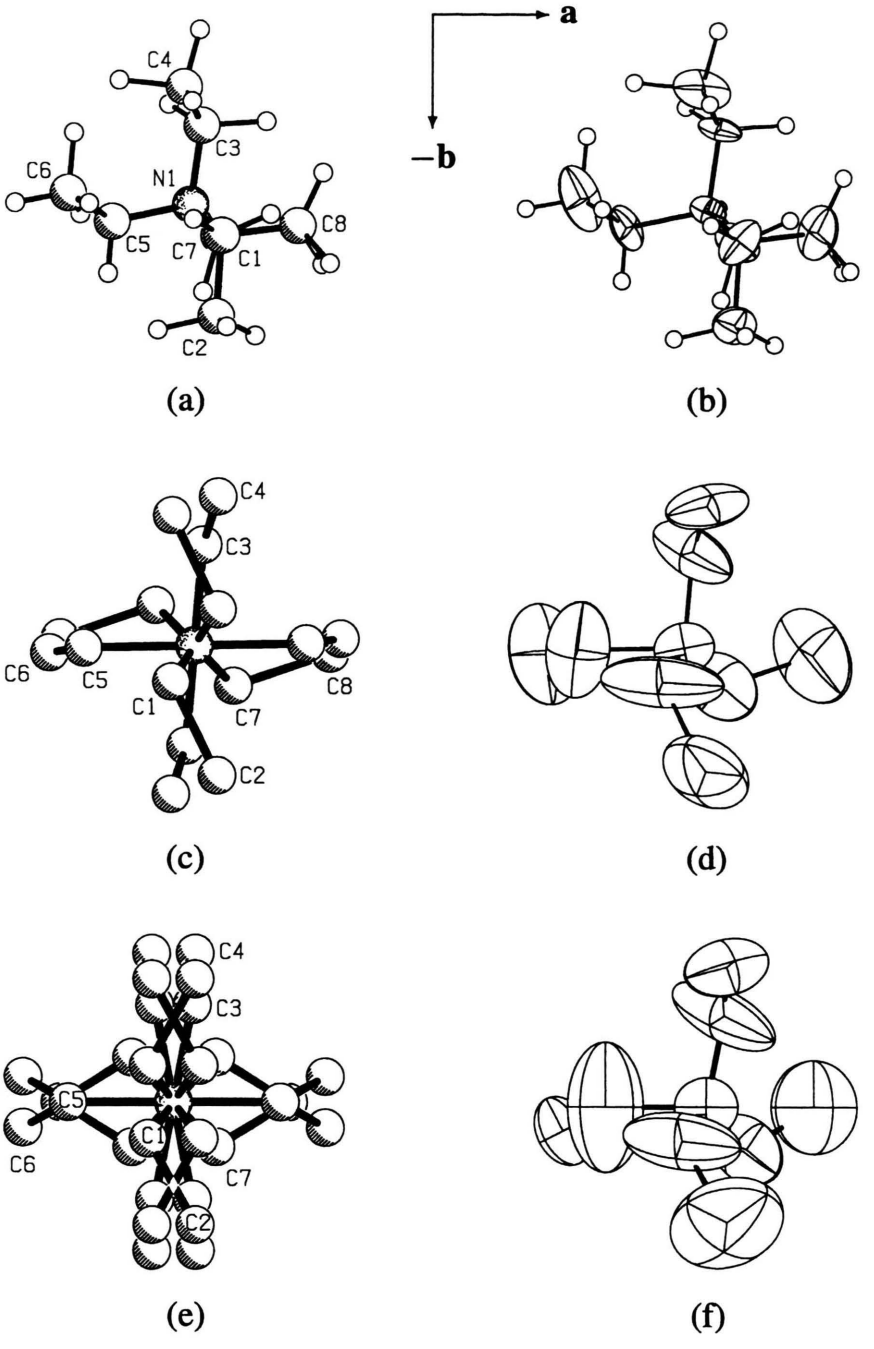

Fig. 5. Ball-stick model with special site symmetry (left) and ORTEP plot of the asymmetric unit (right) of the Et_4N^+ ion in the phases 1–3 of $(Et_4N)_2ZnBr_4$, looking along the basis vector ***c***. The figures (a) and (b) belong to phase 1, (c) and (d) to phase 2, and (e) and (f) to phase 3.

ed. Within the stability range of phase 1, i.e. between 77 and 204 K, three signals with a ratio of the intensities of 1 : 2 : 1 in the order of decreasing frequency ($\nu_1 > \nu_2 > \nu_3$) were observed. Above 204 K these signals fade out. This effect does not coincide with any heat anomaly in the DSC measurements. Therefore no structural phase transition can be attributed to the temperature region around 204 K. On heating up to this temperature the frequency of each of the three signals decreases along with an increase of the amplitude of thermal vibrations. Table 5

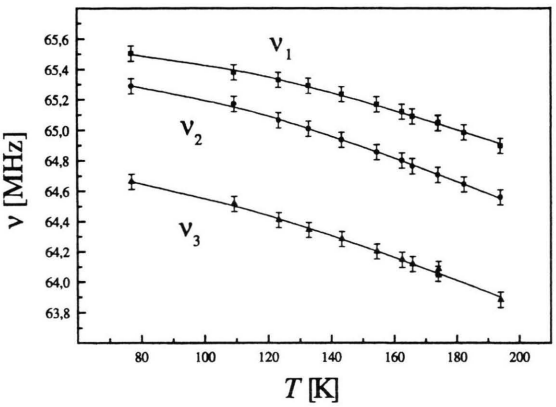

Fig. 6. Temperature dependence of the frequencies of the observed ^{81}Br NQR signals.

shows the results of the polynomial fit to the curves. In general, the number of ^{81}Br NQR signals corresponds to the number of symmetrically independent Br sites and the intensity ratio of these signals to the ratio of the number of different NQR sensitive nuclei, i.e. in this case to the ratio of the corresponding site occupation factors. The number of the three NQR signals and the ratio of their intensities can only be explained by one symmetrically independent $[ZnBr_4]^{2-}$ ion situated on a mirror plane, i.e. a fragment of three Br and one Zn site per asymmetric unit. As can be seen from Fig. 4, this is definitely true for the partial structure of the $[Zn(1)Br_4]^{2-}$ ions at 240 K with the mirror plane oriented perpendicular to the basis vector $\boldsymbol{a}$ of the pseudo-orthorhombic cell, even though the true space group of phase 1 is $P1a1$ because of the lower symmetry of the rest of the structure. The NQR signals that should appear because of the $[ZnBr(2)_4]^{2-}$ ions might be hidden due to crystal field fluctuations.

Discussion

The phase sequence phase 1 → phase 2 → phase 3 of $(Et_4N)_2ZnBr_4$ is essentially characterised by a stepwise increase of the orientational disorder of the Et_4N^+ ion. NMR measurements on $(Et_4N)_2ZnCl_4$ by Wolthuis et al. [15] can be interpreted in terms of a dynamical disorder of the Et_4N^+ ion starting at around 200 K. Similar dynamical processes may appear in the analogous compound $(Et_4N)_2ZnBr_4$. The fading out of the NQR signals in $(Et_4N)_2ZnBr_4$ above 204 K can be correlated with the methyl groups of the Et_4N^+ starting to rotate around the C–C bond axes, though with the hydrogen atoms still preferring the staggered conformation. This is in agreement with the fact that the methyl hydrogen atoms could be located from our D9/D19 neutron data of phase 1 at 240 K. Nevertheless, the equivalent displacement parameters of several of these methyl hydrogen atoms turned out to be rather large (0.10–0.13). A dynamical character of this disorder might also explain the high values of some of the anisotropic displacement parameters of the inner carbon atoms (Fig. 5 (d) and (f)) of this ion. The orientations of the resulting cigar-shaped thermal ellipsoids indicate the approximate directions of movement of these atoms. Besides, it is clear that the diffraction techniques applied always give a time-averaged picture of the structure. The movements of the carbon atoms thus make the Et_4N^+ ion look distorted. The split positions of the outer carbons are rather close to one another in the two disordered phases. The average values of these positions do not deviate much from the positions of the ordered Et_4N^+ ion in phase 1. The increasing disorder of the Et_4N^+ ions on heating up also affects the positions of the heavy atoms. Like the Et_4N^+ ions, the $[ZnBr_4]^{2-}$ ions should be twofold (phase 2) and fourfold (phase 3) disordered. An attempt to resolve the split positions of the Br atoms revealed that they must be very close to one another (≤ 0.5 Å). The fact that the structural changes during the phase sequence phase 1 → phase 2 → phase 3 essentially affect only the positions of the inner carbons explains the close structural relation between the three phases involved. Since the centres of gravity of the central atoms of the Et_4N^+ and the $[ZnBr_4]^{2-}$ ions change only slightly during the transitions, the lattice can be pseudo-orthorhombic in the ordered phase 1.

From the group-subgroup relations of the three phases (Fig. 3) it follows that $(Et_4N)_2ZnBr_4$ crystals are merohedral inversion twins in phase 2. Phase 1, by contrast, is characterised, beside inversion twinning, by reticular pseudo-merohedral reflection twinning with twin planes

$\|(1\ 1\ 0)$ and $(1\ \bar{1}\ 0)$. The definition of the twin planes refers to the common tetragonal lattice of phases 2 and 3. Another twin element, namely a twofold twin axis $\| \boldsymbol{c}^*$, follows from the two twin planes. The more or less equal distribution of the different types of domains in the twinned phases 1 and 2, the slight lattice distortions and remarkable positional changes of the inner carbon atoms only during the two transitions phase 3 → phase 2 and phase 2 → phase 1 explain the occurrence of pseudo-extinction rules, The extinction rules of phase 1, combined with the pseudo-orthorhombic lattice fit well to space group Pma2, the minimal supergroup of the structure of phase 1. The partial structure of the $[Zn(1)Br_4]^{2-}$ ions fulfils the symmetry of this space group with the $[Zn(1)Br_4]^{2-}$ co-ordination polyhedron lying on the mirror plane perpendicular to the basis vector $\boldsymbol{a}$. This is in accordance with the $^{79,81}Br$ NQR results indicating this mirror plane symmetry. The extinction rules of phase 2 fit well to the minimal supergroup $P4_2/nmc$ of the structure of phase 2 and are thus also pretending a higher space group symmetry than is actually present.

Additional information is given by the DSC results (Table 2). The ratio $\omega_{i+1}:\omega_i$ of 8.2:1 of transition 1 (phase 1 ⇌ phase 2) is close to the expected ideal ratio 8:1 and thus confirms the assumption that phase 1 really consists of eight different twin components and that in this case the transformation entropy is dominated by the configurational contribution. The ratio $\omega_{i+1}:\omega_i$ of transition 2 (phase 2 ⇌ phase 3) must be 1:1 because no peak, but only a step was observed in the temperature dependence of the heat flow. Both transitions seem totally reversible. By contrast, the transformation entropies of transition 3 (phase 3 ⇌ phase 4) on heating and on cooling, respectively, differ enormously from one another. Nevertheless, several repetitions of the DSC experiment revealed that the transformation process involved must be totally reversible, too. It is reasonable to assume that the Et_4N^+ ion is even more disordered in phase 4 than it is in phase 3, possibly resulting in a transformation enthalpy which is in accordance with a ratio $\omega_{i+1}:\omega_i$ of ideally 4:1, provided that the transformation enthalpy is approximately equal to the configurational contribution of transition 3 in the direction phase 3 → phase 4 (heating mode).

Support of this work by the Fonds der Chemischen Industrie and Deutsche Forschungsgemeinschaft is gratefully acknowledged.

[1] H. Z. Cummins, Phys. Rep. **185,** 211 (1990).
[2] R. P. A. R. van Kleef, Th. Rasing, J. H. M. Stoelinga, and P. Wyder, Solid State Commun. **39,** 433 (1981).
[3] T. Yamaguchi, S. Sawada, M. Takashige, and T. Nakamura, J. Appl. Phys. **21,** L57 (1982).
[4] K. Nomoto, T. Atake, B. K. Chaudhuri, and H. Chihara, J. Phys. Soc. Japan **52,** 3475 (1983).
[5] K. Hasebe, H. Mashiyama, S. Tanisaki, and K. Gesi, J. Phys. Soc. Japan **51,** 1045 (1982).
[6] K. Hasebe, H. Mashiyama, and S. Tanisaki, J. Appl. Phys. **24,** Suppl 2, 758 (1985).
[7] A. Xenopoulos, J. Cheng, M. Yasuniwa, and B. Wunderlich, Mol. Cryst. Liq. Cryst. **214,** 63 (1992).
[8] G. D. Stucky, J. B. Folkers, and T. J. Kistenmacher, Acta. Cryst. **23,** 1064 (1967).
[9] S. Sveleba, V. Mokryi, I. Polovinko, V. Kapustyanik, Z. Trybula, P. Petrenko, G. Kiosse, and V. Kravtsov, Acta Phys. Pol. A **83 (6),** 777 (1993).
[10] M. Kahrizi, M. O. Steinitz, and T. Smith-Palmer, Solid State Commun. **77 (2),** 99 (1991).
[11] O. G. Vlokh, I. I. Polovinko, V. I. Mokryi, and S. A. Sveleba, Kristallografiya **36,** 227 (1991).
[12] M. Geselle and H. Fuess, Acta Cryst. **C50,** 1582 (1994).
[13] G. M. Sheldrick, SHELX-97, program package for the determination of crystal structures, University of Göttingen, Germany 1997.
[14] H. Bärnighausen, Comm. Math. Chem. **9,** 139 (1980).
[15] A. J. Wolthuis, W. J. Huiskamp, L. J. De Jongh, and R. L. Carlin, Physica **142 B,** 301 (1986).